THE JOURNAL OF BIOLOGICAL CHEMISTRY VOL. 289, NO. 20, pp. 14351–14359, May 16, 2014

Cysteine Palmitoylation of the γ Subunit Has a Dominant Role in Modulating Activity of the Epithelial Sodium Channel*

Received for publication, October 9, 2013, and in revised form, March 28, 2014 Published, JBC Papers in Press, April 1, 2014, DOI 10.1074/jbc.M113.526020

Anindit Mukherjee[‡1], Gunhild M. Mueller[‡1], Carol L. Kinlough[‡], Nan Sheng[‡], Zhijian Wang[‡], S. Atif Mustafa[‡], Ossama B. Kashlan[‡], Thomas R. Kleyman[‡§2], and Rebecca P. Hughey[‡§¶]

From the [‡]Renal-Electrolyte Division, Department of Medicine, and [§]Department of Cell Biology, [¶]Department of Microbiology and Molecular Genetics, University of Pittsburgh, Pittsburgh, Pennsylvania 15261

Background: Epithelial sodium channel (ENaC) β and γ subunits are modified by Cys palmitoylation.
Results: Palmitoylation of the γ subunit activates ENaCs by increasing channel open probability.
Conclusion: γ subunit palmitoylation has a dominant role in activating ENaCs compared with β subunit palmitoylation.
Significance: ENaC palmitoylation is an important post-translational mechanism of channel regulation.

The epithelial sodium channel (ENaC) is composed of three homologous subunits (α, β, and γ) with cytoplasmic N and C termini. Our previous work revealed that two cytoplasmic Cys residues in the β subunit, βCys-43 and βCys-557, are Cys-palmitoylated. ENaCs with mutant βC43A/C557A exhibit normal surface expression but enhanced Na^+ self-inhibition and reduced channel open probability. Although the α subunit is not palmitoylated, we now show that the two cytoplasmic Cys residues in the γ subunit are palmitoylated. ENaCs with mutant γC33A, γC41A, or γC33A/C41A exhibit reduced activity compared with wild type channels but normal surface expression and normal levels of α and γ subunit-activating cleavage. These mutant channels have significantly enhanced Na^+ self-inhibition and reduced open probability compared with wild type ENaCs. Channel activity was enhanced by co-expression with the palmitoyltransferase DHHC2 that also co-immunoprecipitates with ENaCs. Secondary structure prediction of the N terminus of the γ subunit places γCys-33 within an α-helix and γCys-44 on a coil before the first transmembrane domain within a short tract that includes a well conserved His-Gly motif, where mutations have been associated with altered channel gating. Our current and previous results suggest that palmitoylation of the β and γ subunits of ENaCs enhances interactions of their respective cytoplasmic domains with the plasma membrane and stabilizes the open state of the channel. Comparison of activities of channels lacking palmitoylation sites in individual or multiple subunits revealed that γ subunit palmitoylation has a dominant role over β subunit palmitoylation in modulating ENaC gating.

Epithelial sodium channels (ENaCs)[3] are members of the ENaC/degenerin family of ion channels characterized by their sensitivity to amiloride and high selectivity for Na^+ and Li^+ over other cations (1). ENaCs have a primary role in the regulation of Na^+ homeostasis and blood pressure in mammals by mediating apical Na^+ transport in the distal nephron of the kidney. Channel activity is modulated by complex, hormonally regulated signaling pathways that affect ENaC membrane trafficking, degradation, and ultimately its residence time at the plasma membrane. ENaC activity is further regulated through changes in channel open probability (P_o) by factors such as mechanical stress induced by tubular flow, extracellular ions (protons, Na^+, and Cl^-), proteolytic release of extracellular inhibitory tracts, cytoplasmic Cys palmitoylation, and inositol phospholipids (1–4).

ENaCs consist of three homologous subunits (α, β, and γ) that likely form a trimer, based on the resolved structure of the related homotrimeric acid-sensing ion channel 1 (ASIC1) (5, 6). Each subunit has two transmembrane domains linked by a large extracellular region, leaving the relatively short N-terminal and C-terminal domains in the cytoplasm. The homology between ENaCs and ASIC1 suggests that ENaCs adopt a fold in the extracellular and transmembrane domains similar to that observed in the ASIC1 structure (5–7). However, the N and C termini are poorly conserved between ENaC subunits and ASIC1 and are absent in resolved ASIC1 structures.

Cys palmitoylation is the reversible attachment of palmitate to cytoplasmic Cys residues on both soluble and transmembrane proteins (8). Palmitoylation of transmembrane proteins usually occurs at sites adjacent to transmembrane domains or clusters of basic residues and can alter (i) interactions of a particular protein domain with the membrane or with membrane-associated proteins, (ii) protein conformation and function, (iii) protein stability or degradation, or (iv) a combination of these. Cys palmitoylation is now recognized as a common post-translational modification that controls membrane trafficking, further post-translational modifications such as phosphorylation, membrane interactions, and protein conformation, and thereby activity of both ion channels and/or their modifiers/adaptors (9).

We previously used fatty acid-exchange chemistry to demonstrate that the β and γ subunits of mouse and human ENaCs are Cys-palmitoylated (4, 10). Interestingly, we did not observe α subunit palmitoylation (4, 10). Two of the five cytoplasmic β subunit Cys residues (βCys-43 and βCys-557) were palmitoylated (4).

* This work was supported, in whole or in part, by National Institutes of Health Grants R01 DK065161, K01 DK078734, and P30 DK079307.
[1] Both authors contributed equally to this work.
[2] To whom correspondence should be addressed: Renal-Electrolyte Division, Dept. of Medicine, University of Pittsburgh School of Medicine, A919 Scaife Hall, 3550 Terrace St., Pittsburgh, PA 15626. Tel.: 412-647-3121; Fax: 412-648-9166; E-mail: kleyman@pitt.edu.
[3] The abbreviations used are: ENaC, epithelial sodium channel; ASIC1, acid-sensing ion channel 1; HBS, HEPES-buffered saline; HG, His-Gly motif; IP, immunoprecipitate; I_{peak}, peak current; I_{ss}, steady-state current; MDCK, Madin-Darby canine kidney; P_o, open probability.

Channels with Ala substitutions at these sites in the β subunit exhibited reduced whole cell currents compared with wild type ENaCs when expressed in *Xenopus* oocytes. The mutant channels had a reduced P_o compared with wild type, but levels of surface expression for mutant and wild type channels were similar. We now report that the two cytoplasmic Cys in the γ subunit (γCys-33 and γCys-41) are palmitoylated. Channels with a mutant γ subunit bearing Ala substitutions at these sites had a reduced P_o, whereas levels of surface expression were similar to wild type channels. Furthermore, co-expression of ENaCs with a specific palmitoyltransferase led to an increase in channel activity that was dependent on these cytoplasmic Cys residues in the β and γ subunits. Altogether, our new findings and previous observations indicate that palmitoylation of either the β or γ subunit of ENaCs enhances channel P_o and that γ subunit palmitoylation has a dominant role in channel activation.

EXPERIMENTAL PROCEDURES

Vectors and Cell Culture—cDNAs for wild type and epitope-tagged mouse ENaC subunits (N-terminal HA and C-terminal V5) were described previously (11, 12). The γ subunit mutations were generated in pCDNA3.1(+) (Invitrogen) using the QuikChange II XL Site-directed Mutagenesis kit (Stratagene) and confirmed by direct sequencing. The cDNA encoding the palmitoyltransferase DHHC2 (DHHC cysteine-rich domain-containing protein 2) with either an N-terminal HA epitope tag (in pEF-Bos-HA) or an N-terminal EGFP epitope tag (in pEGFP-C1 from BD Biosciences) was a gift from Masaki Fukata (National Institute for Physiological Sciences, Okazaki, Japan) (13). The HA-DHHC2 cDNA was subcloned into pCDNA 3.1(−)neo. The DHHC2 mutant C156S was generated using the QuikChange II XL Site-directed Mutagenesis kit and confirmed by direct sequencing. cRNAs were prepared using mMESSAGE mMACHINE® kit (Ambion Invitrogen). Madin-Darby canine kidney (MDCK) type 2 cells were obtained from Gerard Apodaca (University of Pittsburgh, Pittsburgh, PA). Cells were cultured and transiently transfected with expression vectors as described previously (12).

Assay for Cys Palmitoylation in MDCK Cells—Cys palmitoylation of ENaC subunits was assessed as described previously using fatty acid-exchange chemistry, where *S*-palmitate is selectively removed by treatment with hydroxylamine and exchanged for biotin (4, 14, 15). ENaCs were transiently expressed in MDCK type 2 cells, with a γ subunit that had an N-terminal HA tag and a C-terminal V5 tag (HA-γ-V5), and α and β subunits that lacked epitope tags. Details of the assay were previously published, and minor changes are detailed here (4). Briefly, cells were plated the day before transfection. The day after transfection cells were extracted at room temperature with a detergent buffer (50 mM Tris-HCl, pH 8, 4 mg/ml deoxycholate, 1% Nonidet P-40) containing protease inhibitor mixture set III (Calbiochem) and *N*-ethylmaleimide to alkylate free Cys residues. αβγENaC was then immunoprecipitated with an agarose-immobilized goat anti-V5 antibody. The immunoprecipitates (IPs) were washed and resuspended into freshly made solutions of either 1 M hydroxylamine-HCl (pH 7.4, 150 mM NaCl, 0.2% Triton X-100) to remove *S*-palmitate, or 1 M Tris-HCl (pH 7.4, 150 mM NaCl, 0.2% Triton X-100) as a control, for 60 min before centrifugation. Pellets were washed and resuspended in EZ-Link® (+)-biotinyl-3-maleimidopropionamidyl-3,6-dioxaoactanediamine (maleimide-PEO2-biotin) to label newly exposed Cys sulfhydryls and incubated for 2 h. The pellets were washed once with 1% Triton X-100 in HEPES-buffered saline (HBS, 0.15 M NaCl in 10 mM HEPES, pH 7.5) and once with 0.01% SDS in HBS. ENaC was released from the beads by heating in 1% SDS in HBS. After centrifugation, the supernatant was moved to a new tube. An aliquot of 10% was reserved to determine the "total IP," and the remainder was mixed with Triton X-100 in HBS and avidin conjugated to agarose to recover biotinylated ENaC subunits. The next day, samples were washed, and the pellet was incubated with sample buffer for SDS-PAGE and immunoblotting with anti-V5 antibodies. On these blots we consistently observed both the immature 93-kDa and mature cleaved 75-kDa γ subunit bands in both the total IP and the biotinylated proteins eluted from the avidin-conjugated beads. As we found that the percentage of the γ subunit that was cleaved was similar for the total IP and the biotinylated γ subunit, we concluded that the biotinylated HA-tagged N-terminal 18-kDa fragment containing the cytoplasmic sites for Cys palmitoylation co-immunoprecipitated with the V5-tagged C-terminal 75-kDa fragment. This is consistent with our previous report that fragments of cleaved channel subunits remained together during immunoprecipitation through a disulfide bridge (12). The percentage of biotinylated γ subunit was calculated for each sample based on the total IP. The difference in the percentage of biotinylated subunit following hydroxylamine treatment and the percentage of biotinylated subunit following Tris treatment (*i.e.* control) represents the percentage of the subunit that was palmitoylated.

Test of γENaC Recovery with Avidin-conjugated Beads—Wild type ENaC was transiently expressed in MDCK type 2 cells, with a γ subunit that had an N-terminal HA tag and a C-terminal V5 tag (HA-γ-V5), and α and β subunits that lacked epitope tags. The day following transfection, the apical surface was labeled with sulfo-NHS-SS-biotin, and the subsequent anti-V5 IP was eluted and incubated overnight with avidin conjugated to agarose as described previously (12). The avidin-conjugated beads were recovered by centrifugation and the supernatant was incubated again overnight with avidin-conjugated beads. The beads from each incubation were washed and heated with SDS-gel sample buffer with β-mercaptoethanol for 10 min at 90 °C prior to SDS-PAGE and immunoblotting with anti-V5 antibodies as described.

Co-expression of DHHC2 with αβγ in MDCK Cells—MDCK type 2 cells were seeded onto 12-well tissue culture plates and transfected the following day with 0.5 μg each of plasmids encoding EGFP-DHHC2 and ENaC subunits (HA-α-V5, HA-β-V5, and HA-γ-V5). Detergent extracts of cells were prepared after 24 h and incubated overnight with either control CL6-Sepharose 6B (Sigma) or agarose-immobilized goat anti-V5 antibody (Bethyl Laboratories, Montgomery, TX) (12). The beads were washed twice with 1% Triton X-100 in HEPES-buffered saline and once with HEPES-buffered saline, before elution into SDS-gel sample buffer (Bio-Rad) containing 0.14 M β-mercaptoethanol and heating for 2 min at 90 °C. After SDS-PAGE and transfer to nitrocellulose, the blot was developed with rabbit anti-GFP antibodies (Molecular Probes) as described previously (12).

Functional Expression and Biochemistry in Xenopus Oocytes—ENaC expression in *Xenopus* oocytes and two-electrode voltage clamp were performed as reported previously (16–18). Oocytes were injected with wild type or mutant subunit cRNAs (0.5–1 ng/subunit). Where noted, αβγ wild type or mutant cRNAs (0.5–1 ng/subunit) were co-injected with 3 ng of the palmitoyltransferase DHHC2 or the mutant DHHC2 C156S cRNA. Electrophysiological measurements were performed at 24 h or 48 h after injection as specified. Subunits bearing N-terminal HA and C-terminal V5 tags were used as noted in the text. The difference in measured current at −100 mV in the absence and presence of amiloride (10 μM) was used to define ENaC-mediated currents. The protocol for harvesting oocytes from *Xenopus laevis* was approved by the University of Pittsburgh Institutional Animal Care and Use Committee.

Sodium Self-inhibition Measurements—To evaluate the Na^+ self-inhibition response, a low [Na^+] bath solution (1 mM NaCl, 109 mM *N*-methyl-D-glucamine, 2 mM KCl, 2 mM $CaCl_2$, 10 mM HEPES, pH 7.4) was rapidly replaced by a high [Na^+] bath solution (110 mM NaCl, 2 mM KCl, 2 mM $CaCl_2$, 10 mM HEPES, pH 7.4) while the oocytes expressing ENaC subunits were continuously clamped at −100 mV. The peak current (I_{peak}) and steady-state current (I_{ss}) were determined as described previously (19). The I_{ss} to I_{peak} ratio was used as a measure of the Na^+ self-inhibition response, with a smaller value indicating greater Na^+ self-inhibition.

Single Channel Recordings—Patch clamp recordings were performed in oocytes expressing wild type or mutant ENaCs as described previously (19, 20). Both pipette and bath solutions were the same as the high [Na^+] solution for testing Na^+ self-inhibition (110 mM NaCl, 2 mM KCl, 2 mM $CaCl_2$, 10 mM HEPES, pH 7.4). Patch clamp was performed with a cell-attached configuration using a PC-One Patch Clamp amplifier (Dagan Corp., Minneapolis, MN) and a DigiData 1322A interface connected to a PC. Patches were clamped at membrane potentials (negative value of pipette potentials) of −40 to −100 mV. pClamp 8 or 10 (Molecular Devices Corporation/MDS Analytical Technologies) was used for data acquisition and analyses. Single channel recordings were acquired at 5 kHz, filtered at 300 Hz by a built-in 4-pole low pass Bessel Filter. P_o was estimated by single channel search function of pClamp 10 from 5-min recordings that contained only two current levels (closed and open states) at a clamping membrane potential of −80 or −100 mV.

Statistical Analyses—Comparisons between groups were performed with Student's *t* test unless noted otherwise in the figure legends. A *p* value of <0.05 was considered significantly different.

RESULTS

ENaC Is Palmitoylated at Two Sites on the γ Subunit—We previously used fatty acid-exchange chemistry to show that the β and γ subunits of mouse and human ENaCs, but not the α subunit, are palmitoylated (4, 10). We used this protocol to assess palmitoylation of mouse ENaCs with mutant β subunits where one or more of the five cytoplasmic Cys were mutated to Ala, and we found that only the two Cys adjacent to the first and second transmembrane domains were palmitoylated (4).

The γ subunit has only two cytoplasmic Cys residues. We used fatty acid-exchange chemistry to determine whether one or both of the γ subunit cytoplasmic Cys residues are palmitoylated. MDCK cells were transiently transfected with wild type α and β subunits (nontagged), and wild type or mutant γ subunits (γC33A, γC41A, or γC33A/C41A) with N-terminal HA and C-terminal V5 epitope tags (HA-γ-V5). Cells were extracted the following day with detergent, and αβγENaC was immunoprecipitated with a goat anti-V5 antibody conjugated to agarose beads. Immunoprecipitated channels attached to beads were treated with either hydroxylamine to remove palmitate or with Tris base as a negative control, and then incubated with maleimide-PEO2-biotin to biotinylate newly exposed Cys sulfhydryl groups. ENaC was eluted from the beads with SDS, 10% was reserved to assess the total immunoprecipitated γ subunit, and the remainder was incubated with avidin-conjugated beads to recover biotinylated (*i.e.* palmitoylated) γ subunits for SDS-PAGE. Immunoblotting with mouse anti-V5 antibodies revealed both a 93-kDa band that we previously showed represents an immature endoglycosidase H-sensitive and noncleaved form of the γ subunit, and a mature 75-kDa band that represents an endoglycosidase H-resistant and furin-cleaved form of the γ subunit (12).

The 93-kDa and 75-kDa bands were found in the total immunoprecipitated and the biotinylated samples, indicating that both the immature (noncleaved) and mature (cleaved) forms of the γ subunit were palmitoylated (Fig. 1*A*, *left*). A control experiment indicated that one precipitation with avidin-conjugated beads was sufficient to recover the biotinylated γ subunit (Fig. 1*A*, *right*). Although sites of γ subunit palmitoylation (γCys-33 and γCys-41) would be present in an N-terminal HA-tagged 18-kDa fragment of the cleaved HA-γ-V5 subunit, and the V5 epitope used to immunoprecipitate the channel is on the C-terminal 75-kDa fragment, our previous work showed that cleaved subunits remain fully associated under the conditions used for immunoprecipitation of the intact channel due to a disulfide bridge (1, 5, 12). The amount of biotinylated γ subunit was calculated as a percentage of the total amount of γ subunit in the anti-V5 immunoprecipitate. This value was calculated for samples treated with either hydroxylamine or Tris. The difference in the percentage of subunit biotinylation following hydroxylamine *versus* Tris treatment represents the percentage of the subunit that was palmitoylated (Fig. 1*B*). In each experiment, the percentage of mutant γ subunit palmitoylation was then normalized to the percentage of wild type γ subunit palmitoylation (set as a value of 1). When data from five experiments were combined, we observed that palmitoylation of only the double mutant γC33A/C41A was significantly reduced compared with wild type γ subunit. These data suggest that the γ subunit of ENaC is palmitoylated at both γCys-33 and γCys-41 adjacent to the first transmembrane domain that begins at Leu-55.

ENaCs Lacking Sites for γ Subunit Palmitoylation Exhibit Reduced Activity—We examined whether the lack of palmitoylation sites at either γCys-33 or γCys-41 affected ENaC activity. We previously found that lack of palmitoylation sites at either βCys-43 or βCys-557 reduced ENaC activity (4). Whole cell amiloride-sensitive Na^+ currents were measured in *Xenopus* oocytes expressing wild type α and β subunits with either wild

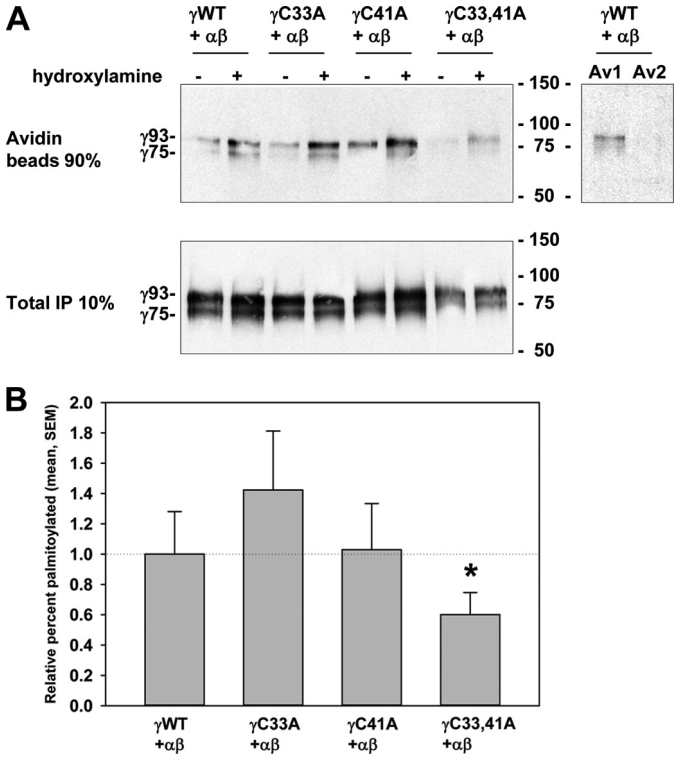

FIGURE 1. **Two γ subunit cytoplasmic Cys residues are palmitoylated.** α and β subunits were co-expressed with a wild type or mutant γ subunit (γWT, γC33A, γC41A, or γC33A/C41A with N-terminal HA and C-terminal V5 tags) in MDCK cells. Cys palmitoylation of the γ subunit in anti-V5 IPs was assessed with fatty acid-exchange chemistry where palmitate is removed with hydroxylamine treatment (+), using Tris treatment as a negative control (−), and replaced with biotin. A fraction was reserved to assess total γ subunit in an initial IP (10%), and biotinylated γ subunit was recovered with avidin-conjugated beads (90% biotin) for immunoblotting with anti-V5 antibodies. Note that the percentage of cleaved HA-γ-V5 subunit (revealed as the C-terminal 75-kDa V5-tagged fragment) is similar between the total IP and that eluted from the avidin-conjugated beads. This is consistent with efficient recovery of biotin-labeled cleaved N-terminal HA-tagged 18-kDa fragment (co-precipitating with the C-terminal V5-tagged 75 kDa fragment), as well as biotin-labeled full-length HA-γ-V5 subunit. The percentage palmitoylated is calculated from the difference in γ subunit biotinylation after treatment with hydroxylamine or Tris, relative to the γ subunit recovered in the total IP. *A*, representative immunoblots are shown with the mobility of the noncleaved (γ93) and cleaved (γ75) γ subunit on the *left*, and Bio-Rad molecular mass markers on the *right*. A control experiment was carried out to ensure that all biotinylated γ subunit was recovered by precipitation with avidin-conjugated beads (*Av1*), as a second incubation with avidin-conjugated beads (*Av2*) revealed no additional γ subunit. *B*, data from multiple experiments are presented as mean ± S.E. (*error bars*, $n = 4–5$) with levels of palmitoylation normalized to channels with a wild type γ subunit (1.0) in each experiment (3.3 ± 0.9% palmitoylated, $n = 5$). Only mutation of both Cys residues (γC33A/C41A) significantly reduced γ subunit palmitoylation (*, $p < 0.05$).

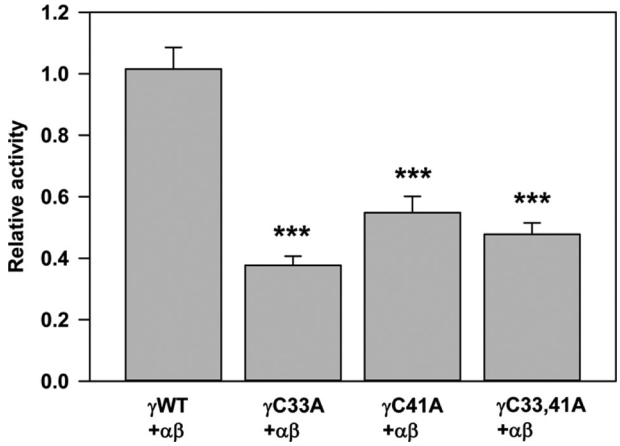

FIGURE 2. **Channels with a γC33A, γC41A, or γC33A/C41A mutant exhibit reduced activity.** Whole cell amiloride-sensitive Na^+ currents were measured in *Xenopus* oocytes expressing nontagged wild type ((αβγ) WT) or channels with mutant γ subunits ($n = 21–27$). Data obtained 24 h after cRNA injections were normalized to wild type channels measured in the same batch of oocytes, and statistically significant differences for the mutants compared with wild type channels are indicated (***, $p < 0.001$ by one-way analysis of variance with Tukey's post hoc test). Data are presented as mean ± S.E. (*error bars*).

type or mutant γ subunits (γC33A, γC41A, or γC33A/C41A). Channels with a single Cys mutation at either site had significantly reduced current compared with wild type ENaCs (Fig. 2). We found that Na^+ currents were not further reduced when both Cys residues were mutated (*i.e.* γC33A/C41A).

The lack of γ subunit palmitoylation sites could reduce ENaC activity either by altering membrane trafficking and affecting the number (*N*) of channels on the cell surface and/or by affecting channel gating and thereby P_o. We first asked whether the lack of palmitoylation sites reduced ENaC expression at the cell surface. Oocytes expressing ENaCs with wild type or mutant γ subunits (γC33A or γC41A) were treated with the membrane-impermeant sulfo-NHS-SS-biotin as described previously (21). Nontagged α and β were co-expressed with HA-γ-V5 (wild type or a γCys mutant), or nontagged β and γ (wild type or a γCys mutant) were co-expressed with HA-α-V5. Ooctyes were extracted with detergent, 2% of the extract was incubated with anti-V5 antibodies conjugated to agarose to assess total α or γ subunit expression, and the remainder was incubated with streptavidin-conjugated agarose to recover surface-biotinylated subunits. Samples were analyzed after SDS-PAGE by immunoblotting with anti-V5 antibodies (Fig. 3*A*). We found no difference in the percentage of ENaC present at the cell surface when γ subunit palmitoylation was blocked by either the γC33A or γC41A mutation, regardless of whether we analyzed levels of the α or γ subunits (Fig. 3*B*). Our results suggest that the reduced activity of ENaCs lacking palmitoylation at γCys-33 or γCys-41 was not due to changes in the number (*N*) of channels on the cell surface.

We then tested the possibility that γ subunit palmitoylation could reduce ENaC activity by reducing ENaC proteolytic cleavage which directly affects channel P_o (3). We therefore evaluated the extent of both α and γ subunit cleavage when palmitoylation of the γ subunit was blocked. Both immature noncleaved (95-kDa α and 93-kDa γ) and mature cleaved (65-kDa α and 75-kDa γ) forms of both the HA-α-V5 and HA-γ-V5 subunits were observed on the surface of oocytes (Fig. 3*A*). Densitometric analysis of the bands revealed that blocking palmitoylation through either the γC33A or γC41A mutation did not affect the extent of cleavage (Fig. 3*C*). We observed a more heterogeneous banding pattern of cleaved γ subunits at the surface of *Xenopus* oocytes compared with the banding pattern of cleaved γ subunits in MDCK cells (compare Fig. 3*A* with Fig. 1*A*). This likely reflects differences in *N*-glycan processing in oocytes and MDCK cells, as we have previously shown that only the cleaved forms of the α and γ subunits have terminally processed *N*-glycans (12, 22). These differences in the banding patterns of cleaved γ subunits are consistent with previously published observations (4, 12, 21–25).

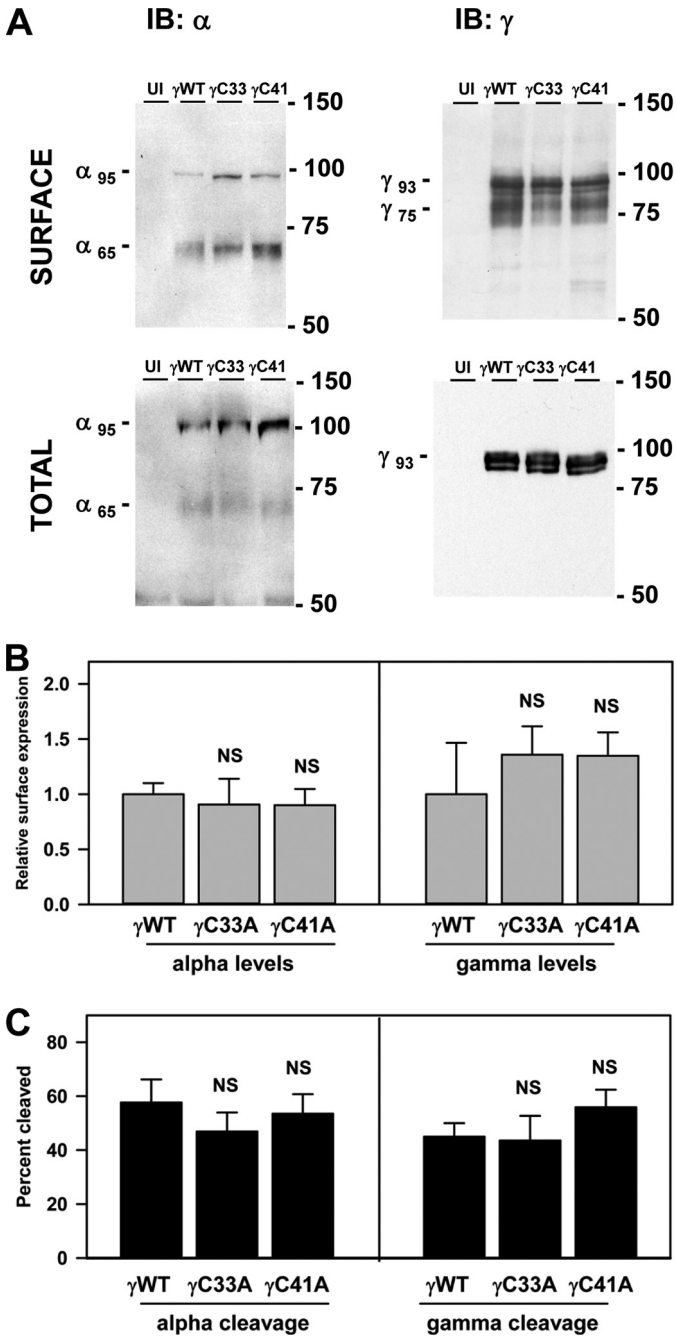

FIGURE 3. **Surface expression and activating cleavage of ENaCs are not altered by the γC33A or γC41A mutation.** Oocytes expressing channels with wild type or mutant γ subunits (γC33A or γC41A) were treated with membrane-impermeant sulfo-NHS-SS-biotin. Nontagged β and γ subunits were co-expressed with a double epitope-tagged α subunit (N-terminal HA and C-terminal V5) to assess α subunit processing. Nontagged α and β subunits were co-expressed with a double epitope-tagged γ subunit (N-terminal HA and C-terminal V5) to assess γ subunit processing. Oocytes were solubilized, 2% of the extract was incubated with anti-V5 antibodies conjugated to beads to measure total α or γ subunit, and surface biotinylated proteins were recovered with streptavidin-conjugated beads. Eluted samples were subjected to SDS-PAGE and immunoblotting (*IB*) with anti-V5 antibodies. Bands on scanned films were analyzed with Bio-Rad Quantity One Software. *A*, representative profiles are shown from one of three experiments. *B*, surface expression of ENaCs with mutant subunits was compared with ENaC with wild type subunits. The levels of surface expression in each experiment were normalized to wild type ENaC. Data are presented as mean ± S.E. (*error bars*; $n = 3$). No statistically significant differences were found (*NS*). *C*, the percentages of mature, cleaved α or γ subunits of surface (*i.e.* biotinylated) ENaCs were determined using the levels of immature noncleaved full-length (α95 kDa and γ93 kDa) and mature cleaved forms (α65 kDa and γ75 kDa) of the subunits. Percentage cleaved = (mature × 100)/(mature + immature). Data are presented as mean and S.E. ($n = 3$). No statistically significant differences were found where indicated (*NS*).

ENaCs Lacking Sites for γ Subunit Palmitoylation Exhibit Enhanced Na^+ Self-inhibition and Reduced Channel P_o—High external [Na^+] reduces channel P_o through a process of Na^+ self-inhibition (1). ENaC P_o correlates well with the degree of Na^+ self-inhibition (26). We reported previously that the reduced activity of ENaCs lacking palmitoylation of the β subunit was due to changes in channel gating leading to a reduced P_o. This occurred in the absence of any changes to cleavage of the channel and was reflected in an enhanced Na^+ self-inhibition response (4). We assessed the Na^+ self-inhibition response of ENaCs lacking γ subunit palmitoylation by monitoring whole cell Na^+ currents of *Xenopus* oocytes in a low [Na^+] bath (1 mM) followed by a rapid change to a high [Na^+] bath (110 mM) (Fig. 4*A*). Following the switch from low to high [Na^+], Na^+ currents rise quickly to a peak (I_{peak}) and then decay to a new steady-state level (I_{ss}). The ratio I_{ss}/I_{peak} reflects the magnitude of the Na^+ self-inhibition response, with a smaller ratio indicating greater Na^+ self-inhibition. We observed that the Na^+ self-inhibition response of ENaCs lacking one or more sites for palmitoylation on the γ subunit was significantly enhanced compared with the Na^+ self-inhibition response of wild type ENaCs (Fig. 4*B*). We performed cell-attached patch clamp studies to determine directly whether ENaCs lacking sites for γ subunit palmitoylation exhibited a reduced P_o (Fig. 5*A*). Whereas wild type ENaCs had an intermediate P_o of 0.35 ± 0.08, αβγC33A and αβγC41A channels had lower P_o values of 0.09 ± 0.02 and 0.19 ± 0.05, respectively (Fig. 5, *B* and *C*). Only the P_o of αβγC33A channels significantly differed from that of wild type channels. These observations show that blocking γ subunit palmitoylation reduced ENaC activity by reducing the channel P_o.

We previously showed that the β subunit is palmitoylated at Cys-43 and Cys-557, and preventing palmitoylation of these residues reduces ENaC activity and P_o. We assessed the activities of wild type ENaC and channels with β subunit Cys mutations (αβC43A/C557Aγ), γ subunit Cys mutations (αβγC33A/C41A), or β and γ subunit Cys mutations (αβC43A/C557A/γC33A/C41A) (Fig. 6). The activity of channels lacking palmitoylation sites due to β subunit Cys mutations was significantly greater than the activity of channels lacking palmitoylation sites due to γ subunit Cys mutations, as well as channels with both β and γ subunit Cys mutations. However, the activities of αβγC33A/C41A and αβC43A/C557A/γC33A/C41A were similar. These results suggest that blocking γ subunit palmitoylation has a dominant effect over blocking β subunit palmitoylation in reducing ENaC activity.

Our cumulative results from studies in MDCK cells and *Xenopus* oocytes, both here and in our previous publication (4), indicate that two Cys in the β subunit and two Cys in the γ subunit are palmitoylated and that blocking palmitoylation of either subunit by mutating these Cys residues reduces ENaC activity. There is a family of 23 palmitoyltransferases (referred to as DHHCs) in humans and mice that catalyze the transfer of

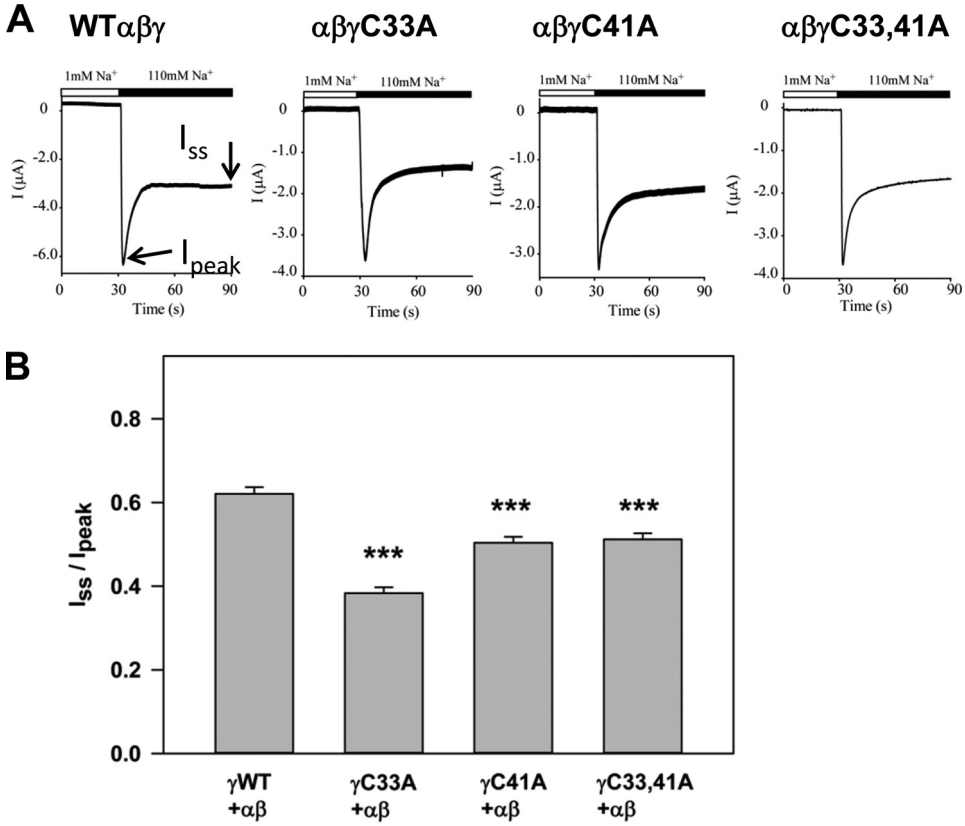

FIGURE 4. **Channels with the γC33A or γC41A mutant exhibit enhanced Na^+ self-inhibition.** *A*, whole cell currents were measured in oocytes expressing ENaCs bathed in a low (1 mM) [Na^+] bath and subsequently with high (110 mM) [Na^+] bath as indicated by the *bar* in the representative tracings. The I_{peak} and the I_{ss} were recorded. ENaCs with γWT, γC33A, and γC41A had N-terminal HA and C-terminal V5 tags, whereas ENaC with γC33A/C41A had no epitope tag. *B*, the ratio of the I_{ss} to the I_{peak} is presented for ENaCs with wild type or mutant subunits as mean ± S.E. (*error bars*) ($n = 16–51$). Statistically significant differences for the mutants compared with wild type channels are indicated (***, $p < 0.001$).

palmitate to specific proteins. To assess the functional role of ENaC palmitoylation directly, we co-expressed ENaC with the palmitoyltransferase DHHC2 in oocytes to determine whether DHHC2 activated ENaC and whether channel activation required the key cytoplasmic Cys residues in the β and γ subunits. As shown in Fig. 7, *A* and *B*, co-expression of wild type mouse ENaC with mouse DHHC2 increased amiloride-sensitive sodium currents by 2.5-fold. However, co-expression of ENaC with DHHC2 where the catalytic domain Cys was mutated to Ser (C156S) did not alter ENaC activity (Fig. 7*B*). In addition, we observed that DHHC2 co-immunoprecipitated with wild type ENaC (Fig. 8). Mutating palmitoylation sites on the β subunit (αβC43A/C557Aγ) significantly reduced the extent of channel activation by DHHC2 (Fig. 7). Moreover, channels lacking palmitoylation sites on the γ subunit (αβγC33A/C41A) or on both the β and γ subunits (αβC43A/C557A/γC33A/C41A) were not activated by DHHC2. These data strongly support our hypothesis that ENaC is palmitoylated on both the β and γ subunits and that palmitoylation increases ENaC activity. In agreement with data in Fig. 6, we observed a greater inhibition of ENaC activity when γ subunit palmitoylation was blocked than when β subunit palmitoylation was blocked, even when palmitoylation was enhanced by co-expression with DHHC2 (compare activities of αβC43A/C557Aγ +DHHC2 with αβγC33A/C41A +DHHC2).

DISCUSSION

Palmitoylation of ENaC Modulates Channel Gating—Our results suggest that the two Cys residues in the N-terminal cytoplasmic tail of the γ subunit of ENaC are palmitoylated and that loss of γ subunit palmitoylation reduces ENaC activity by reducing channel P_o. Although we observed a significant reduction in γ subunit palmitoylation only when both γCys-33 and γCys-41 were mutated, loss of the palmitoylation sites at either γCys-33 or γCys-41 significantly reduced ENaC activity, consistent with a functional role for palmitoylation of either of these γ subunit Cys residues.

The assay for γ subunit palmitoylation is complicated by the fact that the γ subunit is cleaved during ENaC maturation. The β subunit is not cleaved during maturation, simplifying our previous analysis of β subunit palmitoylation. Cleavage of the double-epitope tagged γ subunit produces a C-terminal V5-tagged 75-kDa fragment and an N-terminal HA-tagged 18-Da fragment, with γCys-33 and γCys-41 located in the smaller fragment. We previously reported that the α, β, and γ subunits, including any cleaved fragments of the α and γ subunits, remain associated after detergent extraction of cultured cells (12, 22). Therefore, we relied on the readout of the C-terminal V5-tagged 75-kDa fragment using immunoblotting as an indicator of cleaved γ subunit palmitoylation and the V5-tagged 93-kDa band as an indicator of non-cleaved γ subunit palmitoylation.

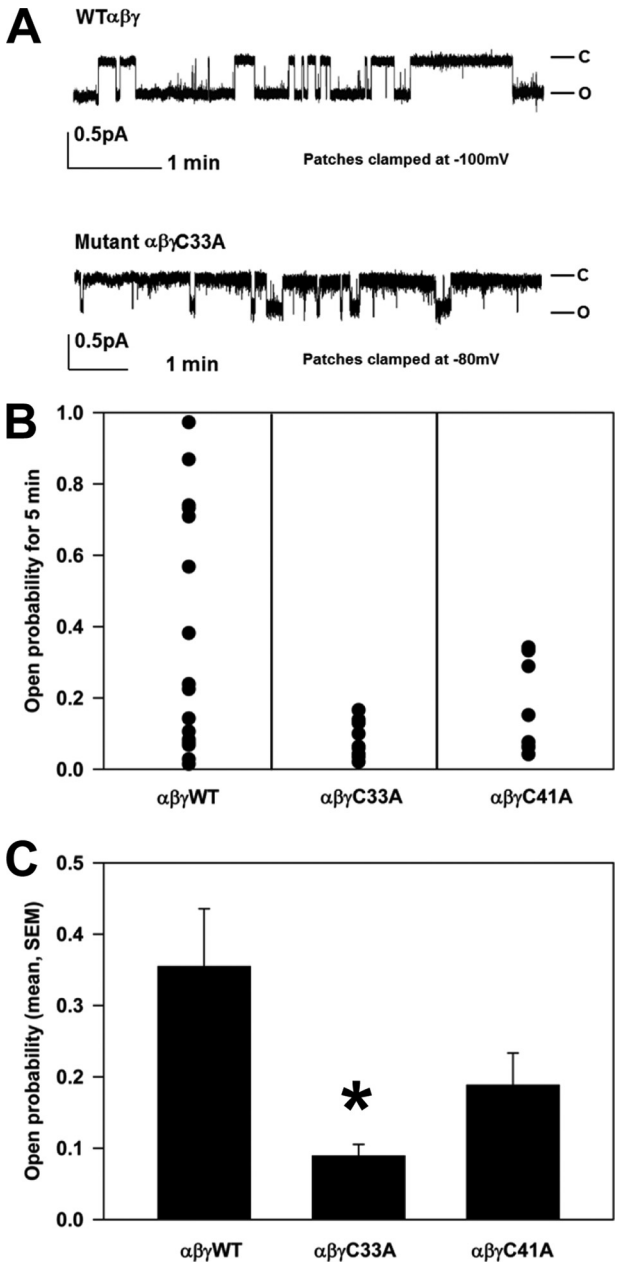

FIGURE 5. **Channels with the mutant γC33A exhibit a reduced P_o.** *A*, cell-attached patch clamp recordings were obtained from oocytes expressing wild type (WT) channels or channels with the γC33A or γC41A mutant. Patches were clamped as indicated. Representative recordings are shown for αβγ and αβγC33A. *B*, recordings of single channels lasting at least 5 min were selected for analysis. *C*, statistical analyses of P_o values for ENaCs with mutant subunits were compared with wild type (*, $p < 0.05$, $n = 9–17$; *error bars*, S.E.).

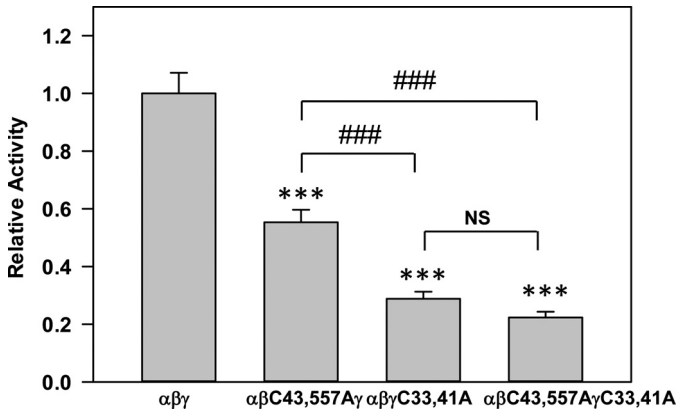

FIGURE 6. **γ subunit palmitoylation has a dominant effect over β subunit palmitoylation on ENaC activity.** Whole cell amiloride-sensitive Na^+ currents were measured in *Xenopus* oocytes expressing wild type ENaC or mutant channels lacking sites for β (αβC43A/C557Aγ) or γ (αβγC33A/C41A) subunit palmitoylation, or lacking palmitoylation sites on both subunits (αβC43A/C557AγC33A/C41A) ($n = 25–43$). All subunits lacked epitope tags. Data obtained 24 h after cRNA injection were normalized to channels with wild type subunits each day, and statistically significant differences between mutant and wild type channels were determined by analysis of variance followed by a Tukey's post hoc test for pairwise comparisons as indicated (***, $p < 0.001$; *error bars*, S.E.). There was also a statistically significant difference in activity between αβC43A/C557Aγ and αβγC33A/C41A, and between αβC43A/C557Aγ and αβC43A/C557AγC33A/C41A (###, $p < 0.001$). There was no statistical (*NS*) difference between αβγC33A/C41A and αβC43A/C557AγC33A/C41A.

γ Subunit Palmitoylation Has a Dominant Role in Activating ENaC—We have shown that preventing ENaC palmitoylation at specific sites in the β or γ subunit, by introducing Cys to Ala substitutions, reduced channel activity. Interestingly, multiple Cys to Ala mutations in a single subunit did not result in a cumulative reduction in channel activity (see Fig. 2 and Ref. 4). When comparing channels with β subunit Cys mutations (αβC43A/C557Aγ), γ subunit Cys mutations (αβγC33A/C41A), and channels with mutations in both subunits (αβC43A/C557AγC33A/C41A) (see Figs. 6 and 7), our results suggested that γ subunit palmitoylation has a dominant role over β subunit palmitoylation in channel activation.

Secondary structural predictions suggest that γCys-33 is within a predicted cytoplasmic N-terminal α-helix, whereas γCys-41 resides between this α-helix and the first transmembrane domain (Fig. 9). The basis for the dominant effect of the γ subunit Cys mutants on ENaC activity (Figs. 6 and 7) is not known, but it is interesting to note that these residues are in close proximity to a highly conserved His-Gly (HG) track that is present in the N-terminal cytoplasmic domains of all ENaC subunits. The importance of the HG track in modulating channel activity was initially revealed by the finding of a missense mutation of the Gly residue in the HG track of the β subunit (βHG37S) in an individual with pseudohypoaldosteronism (27). Gly mutations in the HG tracks of the human α (αG95S), β (βG37S), or γ (γG40S) subunits significantly reduced ENaC activity, likely by reducing channel P_o (27). Analyses of rat ENaCs with mutations in the α subunit revealed that a stretch of consecutive amino acids, including the HG track, influenced channel activity (28). Based on these observations, it is likely that palmitoylation of Cys residues in proximity to the HG track of the γ subunit would also affect channel P_o. The resolved structures of ASIC1 in nonconducting and conducting states suggest that there is movement of the pore-forming transmembrane domains of ASIC1 in association with transitions between functional states (29). If ENaC transmembrane domains undergo similar movements when transitioning between functional states, it is likely that tethering the region preceding the first transmembrane domain of the γ subunit to the membrane as a result of palmitoylation would affect channel gating.

Prediction tools (*e.g.* CSS-Palm 2.0) suggest that >50% of human ion channels may be modified by palmitoylation. A

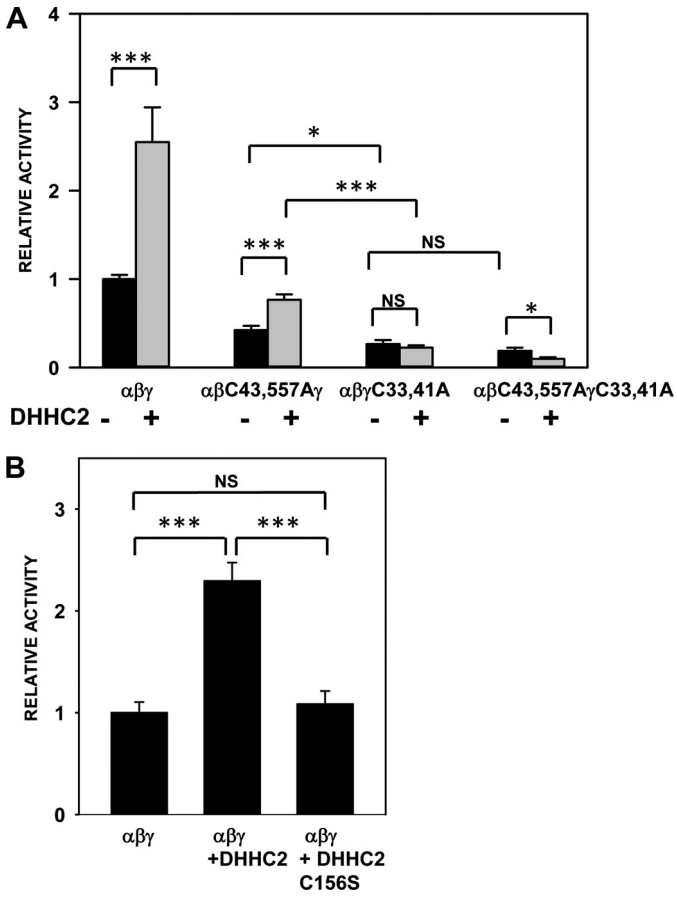

FIGURE 7. **ENaC activity is enhanced by co-expression of a palmitoyltransferase.** *A*, whole cell amiloride-sensitive Na^+ currents were measured in *Xenopus* oocytes expressing nontagged ENaC with either wild type subunits, mutant β subunit ($\alpha\beta$C43A/C557Aγ), mutant γ subunit ($\alpha\beta\gamma$C33A/C41A), or both mutant β and γ subunits ($\alpha\beta$C43A/C557AγC33A/C41A) ($n = 14–51$), with or without DHHC2. Amiloride-sensitive Na^+ currents obtained 48 h after injection of cRNAs were normalized to currents measured in oocytes expressing wild type channels in the same batch. Data are presented as mean ± S.E. (*error bars*). Statistically significant differences with and without DHHC2 expression were observed for wild type $\alpha\beta\gamma$ (***, $p < 0.0001$), $\alpha\beta$C43A/C557Aγ (***, $p < 0.0001$), and $\alpha\beta$C43A/C557AγC33A/C41A (*, $p < 0.05$). DHHC2 did not alter $\alpha\beta\gamma$C33A/C41A currents (*NS*, not significant). Statistically significant differences were also observed for wild type $\alpha\beta\gamma$ + DHHC2 *versus* $\alpha\beta$C43A/C557Aγ + DHHC2 ($p < 0.001$), $\alpha\beta\gamma$ + DHHC2 *versus* $\alpha\beta\gamma$C33A/C41A + DHHC2 ($p < 0.001$), and $\alpha\beta\gamma$ + DHHC2 *versus* $\alpha\beta$C43A/C557AγC33A/C41A + DHHC2 ($p < 0.0001$) (not illustrated in the figure). Statistically significant differences were observed for $\alpha\beta$C43A/C557Aγ *versus* $\alpha\beta\gamma$C33A/C41A (*, $p < 0.05$) and $\alpha\beta$C43A/C557Aγ + DHHC2 *versus* $\alpha\beta\gamma$C33A/C41A + DHHC2 (***, $p < 0.0001$) but not for $\alpha\beta\gamma$C33A/C41A *versus* $\alpha\beta$C43A/C557AγC33A/C41A (*NS*). Statistically significant differences were also observed between $\alpha\beta$C43A/C557Aγ + DHHC2 *versus* $\alpha\beta$C43A/C557AγC33A/C41A + DHHC2 ($p < 0.0001$), and $\alpha\beta\gamma$C33A/C41A + DHHC2 *versus* $\alpha\beta$C43A/C557AγC33A/C41A + DHHC2 ($p < 0.001$) (not illustrated in the figure). *B*, whole cell amiloride-sensitive Na^+ currents were measured in *Xenopus* oocytes expressing nontagged wild type ENaC subunits alone or ENaC subunits co-expressed with either DHHC2 or the mutant DHHC (C156S) ($n = 28–32$). Amiloride-sensitive Na^+ currents obtained 48 h after injection of cRNAs were normalized to currents measured in oocytes expressing only wild type channels in the same batch. Statistically significant differences were observed when $\alpha\beta\gamma$ was expressed with DHHC2 (**, $p < 0.001$), but not with mutant DHHC2 (*NS*, not significant). *Error bars*, S.E.

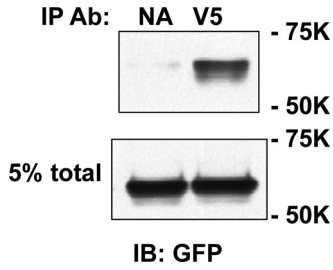

FIGURE 8. **DHHC2 co-immunoprecipitates with ENaC.** Extracts of MDCK cells transfected with enhanced GFP-tagged DHHC2 (FW 71,350) and $\alpha\beta\gamma$ENaC (all three subunits had C-terminal V5 epitope tags) were incubated with anti-V5-conjugated beads (*V5*) or control beads with no antibody (*NA*), and immunoprecipitates were immunoblotted with anti-GFP antibodies (*Ab*; *IB: GFP*). An aliquot of each cell extract (5%) was retained as "total." Mobility of Bio-Rad molecular mass markers are on the *right* of the gel.

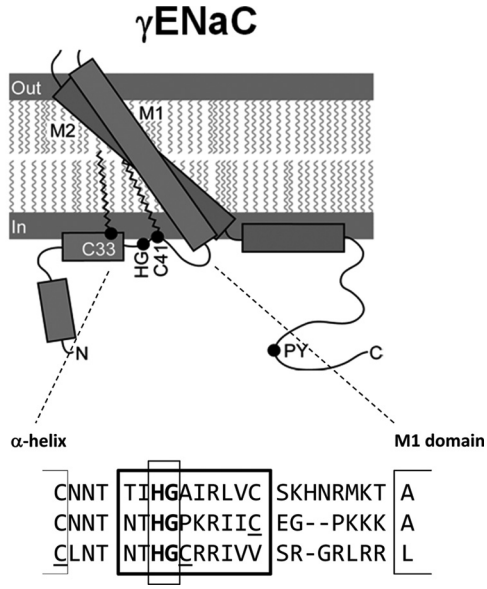

FIGURE 9. **Model of sites of γ subunit palmitoylation.** *A*, the rotation, angle, and length of the transmembrane domains 1 ((TM1) γLeu-55 to Ile-102) and 2 ((TM2) γAsn-528 to Phe-560) are based on the resolved structure of ASIC1 (5, 6). These domains are represented as *rectangles* (*M1* and *M2*, respectively). The N-terminal His-Gly (HG) and C-terminal Pro-Tyr (PY) motifs are located at the indicated positions. Palmitate is indicated within the inner leaflet of the membrane as a *wavy line*. The presence of α-helices in the cytoplasmic domains, also represented as rectangles, was predicted using the PROF program (online). Two α-helix structures are predicted in the γ subunit cytoplasmic N terminus that include γGly-4 to Lys-13 and γThr-24 to Cys-33, placing γCys-33 at the terminus of an α-helix. γCys-41 is located between this α-helix and TM1. An α-helix is also predicted immediately following TM2 for the γ subunit (γIle-561 to Ala-580). It may represent a continuation of TM2 into the intracellular space, or exist as a distinct α-helix as depicted. *B*, alignment of mouse α, β, and γ subunit sequences within the N-terminal cytoplasmic domains, noting the HG motif (*bolded*) and surrounding residues. Palmitoylated βCys-43, γCys-33, and γCys-41 are *underlined*.

review of channels that that undergo this type of post-translational modification indicates that the mechanisms of channel regulation by palmitoylation are diverse (9, 30). It was significant to note that palmitoylation of each of the two cytoplasmic Cys residues in the β or γ subunit functions to stabilize the open state of the channel. Cys palmitoylation is a reversible post-translational modification that is thought to increase the affinity of the modified protein for membrane association as originally noted with soluble cytoplasmic proteins (8). There is a family of 23 palmitoyltransferases in humans that catalyze palmitate addition. Members of this family have common structural features, including four transmembrane domains and a catalytic site with a DHHC cysteine-rich domain (Asp-His-His-Cys). Family members vary greatly in size, substrate specificity, interaction with effector proteins, subcellular localization, and tissue expression (31–33). Little is known about the enzymes that remove palmitate, although two relevant cyto-

plasmic acylprotein thioesterases (APT-1 and APT-2) have now been identified (34). The palmitoyltransferase(s) and thioesterase(s) that regulate reversible ENaC palmitoylation have not yet been defined.

We found that co-expression of ENaC with a specific palmitoyltransferase (DHHC2) significantly increased channel activity and that this is largely or completely prevented when channels lack β or γ palmitoylation sites, respectively, or when the DHHC motif is mutated to DHHS (C156S) (Fig. 7). We also found that DHHC2 co-immunoprecipitated with the channel (Fig. 8), raising the possibility that these proteins may be present in a multiprotein complex. In summary, our new results and previous observations provide strong evidence for a role of palmitoylation in regulating ENaC P_o and that γ subunit palmitoylation has a dominant role in channel activation.

REFERENCES

1. Kashlan, O. B., and Kleyman, T. R. (2011) ENaC structure and function in the wake of a resolved structure of a family member. *Am. J. Physiol. Renal Physiol.* **301,** F684–696
2. Satlin, L. M., Carattino, M. D., Liu, W., and Kleyman, T. R. (2006) Regulation of cation transport in the distal nephron by mechanical forces. *Am. J. Physiol. Renal Physiol.* **291,** F923–931
3. Kleyman, T. R., Carattino, M. D., and Hughey, R. P. (2009) ENaC at the cutting edge: regulation of epithelial sodium channels by proteases. *J. Biol. Chem.* **284,** 20447–20451
4. Mueller, G. M., Maarouf, A. B., Kinlough, C. L., Sheng, N., Kashlan, O. B., Okumura, S., Luthy, S., Kleyman, T. R., and Hughey, R. P. (2010) Cys-palmitoylation of the β subunit modulates gating of the epithelial sodium channel. *J. Biol. Chem.* **285,** 30453–30462
5. Jasti, J., Furukawa, H., Gonzales, E. B., and Gouaux, E. (2007) Structure of acid-sensing ion channel 1 at 1.9 Å resolution and low pH. *Nature* **449,** 316–323
6. Gonzales, E. B., Kawate, T., and Gouaux, E. (2009) Pore architecture and ion sites in acid-sensing ion channels and P2X receptors. *Nature* **460,** 599–604
7. Kashlan, O. B., Adelman, J. L., Okumura, S., Blobner, B. M., Zuzek, Z., Hughey, R. P., Kleyman, T. R., and Grabe, M. (2011) Constraint-based, homology model of the extracellular domain of the epithelial Na^+ channel α subunit reveals a mechanism of channel activation by proteases. *J. Biol. Chem.* **286,** 649–660
8. Linder, M. E., and Deschenes, R. J. (2007) Palmitoylation: policing protein stability and traffic. *Nat. Rev. Mol. Cell Biol.* **8,** 74–84
9. Shipston, M. J. (2011) Ion channel regulation by protein palmitoylation. *J. Biol. Chem.* **286,** 8709–8716
10. Mueller, G. M., Yan, W., Copelovitch, L., Jarman, S., Wang, Z., Kinlough, C. L., Tolino, M. A., Hughey, R. P., Kleyman, T. R., and Rubenstein, R. C. (2012) Multiple residues in the distal C terminus of the α-subunit have roles in modulating human epithelial sodium channel activity. *Am. J. Physiol. Renal Physiol.* **303,** F220–228
11. Ahn, Y. J., Brooker, D. R., Kosari, F., Harte, B. J., Li, J., Mackler, S. A., and Kleyman, T. R. (1999) Cloning and functional expression of the mouse epithelial sodium channel. *Am. J. Physiol.* **277,** F121–129
12. Hughey, R. P., Mueller, G. M., Bruns, J. B., Kinlough, C. L., Poland, P. A., Harkleroad, K. L., Carattino, M. D., and Kleyman, T. R. (2003) Maturation of the epithelial Na^+ channel involves proteolytic processing of the α- and γ-subunits. *J. Biol. Chem.* **278,** 37073–37082
13. Fukata, M., Fukata, Y., Adesnik, H., Nicoll, R. A., and Bredt, D. S. (2004) Identification of PSD-95 palmitoylating enzymes. *Neuron* **44,** 987–996
14. Drisdel, R. C., Alexander, J. K., Sayeed, A., and Green, W. N. (2006) Assays of protein palmitoylation. *Methods* **40,** 127–134
15. Drisdel, R. C., and Green, W. N. (2004) Labeling and quantifying sites of protein palmitoylation. *BioTechniques* **36,** 276–285
16. Carattino, M. D., Hill, W. G., and Kleyman, T. R. (2003) Arachidonic acid regulates surface expression of epithelial sodium channels. *J. Biol. Chem.* **278,** 36202–36213
17. Carattino, M. D., Sheng, S., Bruns, J. B., Pilewski, J. M., Hughey, R. P., and Kleyman, T. R. (2006) The epithelial Na^+ channel is inhibited by a peptide derived from proteolytic processing of its α subunit. *J. Biol. Chem.* **281,** 18901–18907
18. Bruns, J. B., Hu, B., Ahn, Y. J., Sheng, S., Hughey, R. P., and Kleyman, T. R. (2003) Multiple epithelial Na^+ channel domains participate in subunit assembly. *Am. J. Physiol. Renal Physiol.* **285,** F600–609
19. Sheng, S., Carattino, M. D., Bruns, J. B., Hughey, R. P., and Kleyman, T. R. (2006) Furin cleavage activates the epithelial Na^+ channel by relieving Na^+ self-inhibition. *Am. J. Physiol. Renal Physiol.* **290,** F1488–1496
20. Carattino, M. D., Sheng, S., and Kleyman, T. R. (2005) Mutations in the pore region modify epithelial sodium channel gating by shear stress. *J. Biol. Chem.* **280,** 4393–4401
21. Bruns, J. B., Carattino, M. D., Sheng, S., Maarouf, A. B., Weisz, O. A., Pilewski, J. M., Hughey, R. P., and Kleyman, T. R. (2007) Epithelial Na^+ channels are fully activated by furin- and prostasin-dependent release of an inhibitory peptide from the γ-subunit. *J. Biol. Chem.* **282,** 6153–6160
22. Hughey, R. P., Bruns, J. B., Kinlough, C. L., and Kleyman, T. R. (2004) Distinct pools of epithelial sodium channels are expressed at the plasma membrane. *J. Biol. Chem.* **279,** 48491–48494
23. Hughey, R. P., Bruns, J. B., Kinlough, C. L., Harkleroad, K. L., Tong, Q., Carattino, M. D., Johnson, J. P., Stockand, J. D., and Kleyman, T. R. (2004) Epithelial sodium channels are activated by furin-dependent proteolysis. *J. Biol. Chem.* **279,** 18111–18114
24. Passero, C. J., Mueller, G. M., Rondon-Berrios, H., Tofovic, S. P., Hughey, R. P., and Kleyman, T. R. (2008) Plasmin activates epithelial Na^+ channels by cleaving the γ subunit. *J. Biol. Chem.* **283,** 36586–36591
25. Passero, C. J., Mueller, G. M., Myerburg, M. M., Carattino, M. D., Hughey, R. P., and Kleyman, T. R. (2012) TMPRSS4-dependent activation of the epithelial sodium channel requires cleavage of the γ-subunit distal to the furin cleavage site. *Am. J. Physiol. Renal Physiol.* **302,** F1–8
26. Maarouf, A. B., Sheng, N., Chen, J., Winarski, K. L., Okumura, S., Carattino, M. D., Boyd, C. R., Kleyman, T. R., and Sheng, S. (2009) Novel determinants of epithelial sodium channel gating within extracellular thumb domains. *J. Biol. Chem.* **284,** 7756–7765
27. Gründer, S., Firsov, D., Chang, S. S., Jaeger, N. F., Gautschi, I., Schild, L., Lifton, R. P., and Rossier, B. C. (1997) A mutation causing pseudohypoaldosteronism type 1 identifies a conserved glycine that is involved in the gating of the epithelial sodium channel. *EMBO J.* **16,** 899–907
28. Gründer, S., Jaeger, N. F., Gautschi, I., Schild, L., and Rossier, B. C. (1999) Identification of a highly conserved sequence at the N terminus of the epithelial Na^+ channel α subunit involved in gating. *Pflugers Arch.* **438,** 709–715
29. Baconguis, I., and Gouaux, E. (2012) Structural plasticity and dynamic selectivity of acid-sensing ion channel-spider toxin complexes. *Nature* **489,** 400–405
30. Ren, J., Wen, L., Gao, X., Jin, C., Xue, Y., and Yao, X. (2008) CSS-Palm 2.0: an updated software for palmitoylation sites prediction. *Protein Eng. Des. Sel.* **21,** 639–644
31. Ohno, Y., Kihara, A., Sano, T., and Igarashi, Y. (2006) Intracellular localization and tissue-specific distribution of human and yeast DHHC cysteine-rich domain-containing proteins. *Biochim. Biophys. Acta* **1761,** 474–483
32. Tsutsumi, R., Fukata, Y., and Fukata, M. (2008) Discovery of protein-palmitoylating enzymes. *Pflugers Arch.* **456,** 1199–1206
33. Korycka, J., Łach, A., Heger, E., Bogusławska, D. M., Wolny, M., Toporkiewicz, M., Augoff, K., Korzeniewski, J., and Sikorski, A. F. (2012) Human DHHC proteins: a spotlight on the hidden player of palmitoylation. *Eur. J. Cell Biol.* **91,** 107–117
34. Tomatis, V. M., Trenchi, A., Gomez, G. A., and Daniotti, J. L. (2010) Acyl-protein thioesterase 2 catalyzes the deacylation of peripheral membrane-associated GAP-43. *PLoS One* **5,** e15045